Available online at www.eccomasproceedia.org
Eccomas Proceedia COMPDYN (2017) 1107-1134

ECCOMAS
Proceedia

COMPDYN 2017
6th ECCOMAS Thematic Conference on
Computational Methods in Structural Dynamics and Earthquake Engineering
M. Papadrakakis, M. Fragiadakis (eds.)
Rhodes Island, Greece, 15–17 June 2017

SEMI-ANALYTICAL REDUCED-ORDER MODELS FOR THE AEROELASTIC BEHAVIOR OF SUBSONIC FLEXIBLE WINGS VIA GENERALISED PLATE AND BEAM FORMULATIONS

Marco Berci

University of Leeds
LS2 9JT, Leeds, UK
M.Berci@leeds.ac.uk

Keywords: reduced-order models, semi-analytical, aeroelasticity, subsonic flexible wings.

Abstract. *Semi-analytical reduced-order models for the combined aeroelastic analysis and gust response of flexible subsonic wings with arbitrary aspect ratio are presented. Both a thin plate and a slender beam are considered as the linear structural dynamics models, within a generalised formulation. A modified strip theory is proposed for modelling the wing unsteady aerodynamics in incompressible flow, accounting for the three-dimensional effects on both spanwise decay and build-up of the airload. Peters' in-flow theory is adopted for calculating the two-dimensional unsteady airload around each morphing wing section, standard and tuned strip theories being readily resumed for comparison and completeness. Considering straight elliptical and trapezoidal planforms, approximate lift-deficiency functions for both a unit step-change in the angle of attack and a unit sharp-edged gust are then employed in place of classic Theodorsen/Wagner's and Sears/Kussner's functions, respectively. A modal approach is finally adopted to write the generalised equations of motion in state-space form, for both plate-based and beam-based formulations. Numerical results are then obtained and critically discussed for the aeroelastic stability analysis of a uniform rectangular wing, with respect relevant aerodynamic and structural parameters. Due to computational efficiency and theoretical insight, the proposed generalised formulation is suggested as an effective aeroelastic tool for the preliminary multidisciplinary design and optimisation (MDO) of flexible wings in the low-subsonic regime, as characterised by incompressible flow.*

Peer-review under responsibility of the organizing committee of COMPDYN 2017.
doi: 10.7712/120117.5480.17045

1 INTRODUCTION

Efficient aeroelastic methods and tools [1-2] based on reduced-order complexity [3-6] are increasingly sought for the preliminary multidisciplinary design and optimisation (MDO) [7-8] of flexible subsonic wings [9-14]. A semi-analytical model for the aeroelastic behavior of a thin straight wing in unsteady incompressible flow is hence here presented. Modified strip theory (MST) is adopted for the aerodynamic load [15-16], tuned strip theory (TST) being readily resumed for comparison and completeness [17-18]. Peters' in-flow theory is adopted for calculating the two-dimensional unsteady airload around each morphing wing section [19], where approximate lift-deficiency functions [20-22] for both a unit step-change in the angle of attack and a unit sharp-edged gust are employed in place of classic Theodorsen/Wagner's and Sears/Kussner's functions [23-28], respectively. Both plate-like and beam-like linear models are considered for the structural dynamics, within a unified formulation [29-30]. The principle of virtual work (PVW) is then used to derive the equilibrium equations and the Ritz's method finally employed to solve them within a modal approach [31-32], where polynomial shape functions are assumed for the wing displacement [33]. The resulting aeroelastic model allows any distribution of the thin wing properties and provides with its continuous deformation [34]. Numerical results for the divergence speeds and flutter frequency [35] of a uniform rectangular wing are finally shown and discussed with respect to the relevant aero-structural parameters such as the aspect and thickness ratios.

2 AEROELASTIC PROBLEM FORMULATION FOR PLATE-LIKE WING

Consider a rectangular flat plate with distributed mass $m(x,y)$ per unit area, moment of inertia $\mu(x,y)$, area moment of inertia $I(x,y)$, torsion factor $J(x,y)$, Young elastic modulus $E(x,y)$, shear modulus $G(x,y)$ and structural damping $\xi(x,y)$; the unsteady airload $\Delta p(x,y,t)$ is also distributed on the entire surface. Being $h(x,y)$ the thickness, c the chord, b the semi-chord and l the semi-span, the $\hat{\mathbf{y}}$ axis of the Cartesian reference system lays on the plate symmetry axis and is directed outward along the span, with $0 \le y \le l$ from clamped root to free tip, whereas the $\hat{\mathbf{x}}$ axis is orthogonal to the plate symmetry axis and directed backward along the chord, with $-b \le x \le +b$ from leading to trailing edge; thus, the vertical $\hat{\mathbf{z}}$ axis is orthogonal to the plate planform and points upward, with $-\frac{h}{2} \le z \le +\frac{h}{2}$ from lower to upper surface. Aspect and thickness ratios then read $AR = \frac{2l}{c}$ and $TR = \frac{h}{c}$, respectively.

Within a linear analysis framework, the plate vertical displacement $w(x,y,t)$ induces a local slope $\boldsymbol{\varsigma}(x,y,t)$ and curvature $\boldsymbol{\theta}(x,y,t)$ readily given at the plate middle surface as $\boldsymbol{\varsigma} = \nabla w$ and $\boldsymbol{\theta} = -\left\{ w^{**} \quad w'' \quad 2w^{*} \right\}^T$, where apices * and ' denote derivation in the x and y directions, respectively. The structural deformation results in strains $\boldsymbol{\varepsilon}(x,y,t)$ and stresses $\boldsymbol{\sigma}(x,y,t)$ which, by employing Kirchhoff's hypothesis and Hook's law [36], read $\boldsymbol{\varepsilon} = \bar{\boldsymbol{\varepsilon}} + z\boldsymbol{\theta}$ and $\boldsymbol{\sigma} = \mathbf{E}\boldsymbol{\varepsilon}$, respectively, where $\mathbf{E}(x,y)$ is the elastic tensor and $\bar{\boldsymbol{\varepsilon}}(x,y)$ is due to pre-stress; for orthotropic material, stiffness and pre-tension matrices can be written as [29-30]:

$$\mathbf{EI}=\begin{bmatrix} EI_x & EI_{xy} & 0 \\ EI_{yx} & EI_y & 0 \\ 0 & 0 & GJ_{xy} \end{bmatrix}, \qquad \mathbf{T}=\begin{bmatrix} \overline{T}_x & \overline{T}_{xy} \\ \overline{T}_{yx} & \overline{T}_y \end{bmatrix}, \tag{1}$$

where the in-plane forces $\overline{T}(x,y)$ and stresses $\overline{\boldsymbol{\sigma}}(x,y)$ are due to pre-loading condition $\overline{\boldsymbol{\sigma}}=\mathbf{E}\overline{\boldsymbol{\varepsilon}}$.

Neglecting gravity and possible concentrated loads (e.g., lumped inertia, spring or damper) without loss of generality, the PVW may readily be written for the arbitrary virtual displacement $\delta w(x,y,t)$ as:

$$\begin{aligned} &\int_0^l\int_{-b}^{+b}\delta\boldsymbol{\theta}^T\mathbf{EI}\,\boldsymbol{\theta}\,dxdy+\int_0^l\int_{-b}^{+b}\delta\boldsymbol{\varsigma}^T\mathbf{T}\boldsymbol{\varsigma}\,dxdy=\int_0^l\int_{-b}^{+b}\delta w\Delta p\,dxdy+\\ &-\int_0^l\int_{-b}^{+b}\delta w\zeta\dot{w}dxdy-\int_0^l\int_{-b}^{+b}\delta wm\ddot{w}dxdy-\int_0^l\int_{-b}^{+b}\delta w^*\mu_x\ddot{w}^*dxdy-\int_0^l\int_{-b}^{+b}\delta w'\mu_y\ddot{w}'dxdy, \end{aligned} \tag{2}$$

and then integrated by parts twice in order to give the linear partial differential equation (PDE) for the dynamic aeroelastic equilibrium [29-30]:

$$\begin{aligned} &\left(EI_xw^{**}+EI_{xy}w''\right)^{**}+4\left(GJ_{xy}w'^*\right)'^*+\left(EI_{yx}w^{**}+EI_yw''\right)''+\left(\overline{T}_xw^*+\overline{T}_{xy}w'\right)^*+\left(\overline{T}_yw'+\overline{T}_{yx}w^*\right)'=\\ &=\Delta p-\zeta\dot{w}-m\ddot{w}+\left(\mu_x\ddot{w}^*\right)^*+\left(\mu_y\ddot{w}'\right)', \end{aligned} \tag{3}$$

which is consistently completed by both geometrical and natural boundary conditions as:

$$\begin{aligned} &w(x,0,t)=0, \qquad w^*(x,0,t)=0, \qquad w'(x,0,t)=0,\\ &EI_xw^{**}\big|_{-b}^{+b}+EI_{xy}w''\big|_{-b}^{+b}=0, \qquad EI_{yx}w^{**}\big|_l+EI_yw''\big|_l=0,\\ &\left(EI_xw^{**}\right)^*\big|_{-b}^{+b}+\left(EI_{xy}w''\right)^*\big|_{-b}^{+b}-\overline{T}_xw^*\big|_{-b}^{+b}-\overline{T}_{xy}w'\big|_{-b}^{+b}-\mu_x\ddot{w}^*\big|_{-b}^{+b}=0,\\ &\left(EI_{yx}w^{**}\right)'\big|_l+\left(EI_yw''\right)'\big|_l-\overline{T}_{yx}w^*\big|_l-\overline{T}_yw'\big|_l-\mu_y\ddot{w}'\big|_l=0,\\ &GJ_{xy}w'^*\big|_{-b}^{+b}=0, \qquad \left(GJ_{xy}w'^*\right)'\big|_{-b}^{+b}=0,\\ &GJ_{xy}w'^*\big|_l=0, \qquad \left(GJ_{xy}w'^*\right)^*\big|_l=0, \end{aligned} \tag{4}$$

as well as the initial rest condition $w(x,y,0)=0$, $w^*(x,y,0)=0$ and $w'(x,y,0)=0$.

2.1 Modal Solution Approach

Rather than solving the governing PDE numerically, the Ritz's method is employed. The plate displacement is then modally expressed as [31-32]:

$$w=\sum_{i=1}^{n}\phi_i\varepsilon_i\,,\qquad\qquad \delta w=\sum_{i=1}^{n}\phi_i\delta\varepsilon_i\,, \tag{5}$$

where the n functions $\varepsilon_i(t)$ are unknown generalised coordinates relative to the n assumed mode shapes $\phi_i(x,y)$, which are hereby chosen as suitable combinations of chordwise $g_k(x)$ and spanwise $f_j(y)$ polynomials satisfying the geometrical boundary conditions for clamped-free plate [31,33], namely:

$$\begin{gathered}\phi_i=g_k f_j\,,\qquad i=kn_j+j\,,\qquad n=n_j(n_k+1),\\ g_k=T_k\left(\frac{x}{b}\right),\qquad 0\le k\le n_k\,,\qquad f_j=\left(\frac{y}{l}\right)^{j+1},\qquad 1\le j\le n_j\,;\end{gathered} \tag{6}$$

note that the chordwise modes are indeed Chebyshev polynomials $\cos(k\Theta)$, with Glauert's transformation $x=b\cos\Theta$ [19,37].

2.2 Generalised Aerodynamic Load

According to thin aerofoil theory [38-39], the sectional unsteady aerodynamic load in incompressible flow is due to the effective angle of attack of the latter with respect to the instantaneous kinematics of the thin wing camber, where the non-penetration boundary condition is imposed assuming small wing deformations and flow perturbations; this includes the unsteady wake inflow. By noting that $w=\sum_{k=0}^{n_k}g_k w_k$ with $w_k=\sum_{j=1}^{n_j}f_j\varepsilon_i$, Peters' model for a morphing thin airfoil is efficiently employed to give the generalised unsteady airload $F_i^a(t)$ as:

$$F_i^a=\int_0^l\int_{-b}^{+b}\Delta p\,\phi_i\,dxdy=\int_0^l\kappa\Delta F_k^a f_j\,dy\,,\qquad\qquad \Delta F_k^a=\int_{-b}^{+b}\Delta p\,g_k\,dx\,, \tag{7}$$

where the wing displacement has effectively been projected onto the chordwise modal base g_k, with the n_k+1 coefficients $w_k(y,t)$ explicitly given by [19]:

$$w_0=\frac{1}{\pi}\int_{-b}^{+b}\frac{w\,dx}{\sqrt{b^2-x^2}}\,,\qquad\qquad w_k=\frac{2}{\pi}\int_{-b}^{+b}\frac{w g_k\,dx}{\sqrt{b^2-x^2}}\qquad k\ge 1; \tag{8}$$

within the framework of a modified strip theory [15-16], the scaling function $\kappa(y)$ accounts for the influence of the wing-tip vortices downwash on the sectional airload and scales the latter proportionally with the local, quasi-steady wing circulation along the span [14].

The generalised unsteady airload for an isolated flexible aerofoil reads [10,19]:

$$\Delta F_0^a=\pi\rho b^2\left(\dot v_0-\frac{\dot v_2}{2}\right)+2\pi\rho bU\mathrm{C}(\mathrm{k})\left(v_0+\frac{v_1}{2}\right)+\Delta F_0^G\,, \tag{9}$$

$$\Delta F_1^a = \frac{\pi}{8}\rho b^2\left(\dot v_1 - \dot v_3\right) + \frac{\pi}{2}\rho bU\left(v_1 + v_2\right) - \pi\rho bU\mathrm{C}(\mathrm{k})\left(v_0 + \frac{v_1}{2}\right) + \Delta F_1^G,$$

$$\Delta F_2^a = -\frac{\pi}{2}\rho b^2\left(\dot v_0 - \frac{2}{3}\dot v_2 + \frac{\dot v_4}{6}\right) - \frac{\pi}{2}\rho bU\left(v_1 - v_3\right),$$

$$\Delta F_k^a = \frac{\pi}{4}\rho b^2\left[\frac{1}{k+1}\left(\dot v_k - \dot v_{k+2}\right) - \frac{1}{k-1}\left(\dot v_{k-2} - \dot v_k\right)\right] - \frac{\pi}{2}\rho bU\left(v_{k-1} - v_{k+1}\right),$$

where ρ is the flow density and $v = \sum_{k=0}^{n_k} g_k v_k$ is the induced flow velocity due to aerofoil motion, the generalised coefficients $v_k(y,t)$ of which are readily given by [10,19]:

$$v_0 = -\dot w_0 - U\sum_{k=1,3}^{n_k}\frac{k w_k}{b}, \qquad v_k = -\dot w_k - 2U\sum_{h=k+1,k+3}^{n_k}\frac{h w_h}{b} \qquad k \geq 1, \tag{10}$$

thus realizing the fluid-structure interaction [40] thru the non-penetration boundary condition. With k the reduced frequency [26-28], $\mathrm{C}(\mathrm{k})$ is the equivalent of Theodorsen's lift-deficiency function for the circulatory lift build-up of a finite wing due to harmonic oscillation and, via Fourier transform [41], is related to the equivalent of Wagner's indicial-admittance function for the circulatory lift build-up due to a unit step in the angle of attack (see Appendix B).

Finally, the airload contribution due to a vertical gust $\mathrm{V_G}(y,t)$, which is here assumed as $\mathrm{V_G} = \Omega V_G$ with spanwise distribution $\Omega(y)$ and time evolution $V_G(t)$, reads [10,32]:

$$\begin{aligned}
\Delta F_0^G &= 2\pi\rho bU\Omega\left(V_{G0}\mathrm{K} + \int_0^t \frac{dV_G(\iota)}{d\iota}\mathrm{K}(t-\iota)d\iota\right),\\
\Delta F_1^G &= -\pi\rho bU\Omega\left(V_{G0}\mathrm{K} + \int_0^t \frac{dV_G(\iota)}{d\iota}\mathrm{K}(t-\iota)d\iota\right),
\end{aligned} \tag{11}$$

where $V_{G0} = V_G(0)$ and $\mathrm{K}(t)$ is the equivalent of Kussner's indicial-admittance function for the circulatory lift build-up of a finite wing due to a unit sharp-edge gust (see Appendix B), assuming a standard "frozen" approach [42].

Note that Peters' theory implicitly assumes the lift-curve slope $C_{L/\alpha} = 2\pi$ for a flat airfoil, which is appropriate for a plate wing; nevertheless, his analytical model can still effectively be tuned with a different value, as long as subsonic potential flow is applicable [11-12]. Finally, the wing lift $L(t)$, pitching moment $M_p(t)$ and rolling moment $M_r(t)$ are given by [18]:

$$L = \int_0^l\int_{-b}^{+b}\Delta p\,dxdy, \qquad M_p = \int_0^l\int_{-b}^{+b}x\Delta p\,dxdy, \qquad M_r = \int_0^l\int_{-b}^{+b}y\Delta p\,dxdy. \tag{12}$$

3 AEROELASTIC PROBLEM FORMULATION FOR BEAM-LIKE WING

According to the closely-spaced rigid diaphragm assumption [36], a slender wing is often considered spanwise flexible only and a beam-like structural model suitably employed [32,34]. As the latter (which is one-dimensional) can be derived from the plate-like structural model (which is two-dimensional), it may be seen as a semi-analytical reduced-order model where the chordwise dependency of the properties is dropped and only the first two chordwise (rigid) modes g_0 and g_1 are implicitly retained [29-30], eventually resulting in two coupled equilibrium equations for bending and torsion [35], respectively.

The wing elastic axis (EA, where all applied loads are reacted [32]) is then modelled as a Rayleigh beam [43] and drawn by the locus of the shear centres of each chordwise section, with $x_{EA}(y)\equiv 0$ fixed for convenience, whereas the inertial axis $x_{CG}(y)$ is drawn by the locus of the sectional centres of gravity (CG, where the inertial load is applied [32]). Thus, we have the distributed mass $m(y)$ per unit length, bending and torsion moment of inertia $\mu_\zeta(y)$ and $\mu_\vartheta(y)$, area moment of inertia $I(y)$, torsion factor $J(y)$, Young modulus $E(y)$, shear modulus $G(y)$, axial tension $\bar{T}(y)$ and bending and torsion structural damping $\xi_\zeta(y)$ and $\xi_\vartheta(y)$.

With $\zeta(y,t)$ and $\vartheta(y,t)$ the vertical and torsional displacements of the elastic axis, respectively, the wing deformation is given as $w=\zeta-x\vartheta$; therefore, neglecting gravity and concentrated loads, the PVW for the arbitrary virtual displacements $\delta\zeta(y,t)$ and $\delta\vartheta(y,t)$ reads:

$$\begin{aligned}&\int_0^l EI\zeta''\delta\zeta''dy+\int_0^l \bar{T}\zeta'\delta\zeta'dy+\int_0^l GJ\vartheta'\delta\vartheta'dy=\int_0^l \Delta L\delta\zeta dy+\int_0^l \Delta M\delta\vartheta dy+\\&-\int_0^l m\ddot{w}_{CG}\delta w_{CG}dy-\int_0^l \mu_\zeta\ddot{w}'_{CG}\delta w'_{CG}dy-\int_0^l \mu_\vartheta\ddot{\vartheta}\delta\vartheta dy-\int_0^l \xi_\zeta\dot{\zeta}\delta\zeta dy-\int_0^l \xi_\vartheta\dot{\vartheta}\delta\vartheta dy,\end{aligned}\tag{13}$$

where $w_{CG}=\zeta-x_{CG}\vartheta$ is the vertical displacement of the inertial axis, whereas $\Delta L(y,t)$ and $\Delta M(y,t)$ are the sectional unsteady aerodynamic force (positive upwards) and pitching moment (positive clockwise), respectively. The virtual displacement being arbitrary, bending and torsion virtual works separate as:

$$\begin{aligned}&\int_0^l EI\zeta''\delta\zeta''dy+\int_0^l \bar{T}\zeta'\delta\zeta'dy=\int_0^l \Delta L\delta\zeta dy+\\&-\int_0^l \xi_\zeta\dot{\zeta}\delta\zeta dy-\int_0^l m\left(\ddot{\zeta}-x_{CG}\ddot{\vartheta}\right)\delta\zeta dy-\int_0^l \mu_\zeta\left(\ddot{\zeta}-x_{CG}\ddot{\vartheta}\right)'\delta\zeta' dy,\\&\int_0^l GJ\vartheta'\delta\vartheta'dy=\int_0^l \Delta M\delta\vartheta dy-\int_0^l \xi_\vartheta\dot{\vartheta}\delta\vartheta dy+\\&-\int_0^l \mu_\vartheta\ddot{\vartheta}\delta\vartheta dy+\int_0^l x_{CG}m\left(\ddot{\zeta}-x_{CG}\ddot{\vartheta}\right)\delta\vartheta dy+\int_0^l x_{CG}\mu_\zeta\left(\ddot{\zeta}-x_{CG}\ddot{\vartheta}\right)'\delta\vartheta' dy,\end{aligned}\tag{14}$$

and are then integrated by parts twice in order to give the linear system of coupled PDEs for the dynamic aeroelastic equilibrium of wing bending and torsion [32] as:

$$\begin{aligned}&\left(EI\zeta''\right)'' - \left(\bar{T}\zeta'\right)' + \xi_\zeta\dot{\zeta} + m\left(\ddot{\zeta} - x_{CG}\ddot{\vartheta}\right) - \mu_\zeta\left(\ddot{\zeta} - x_{CG}\ddot{\vartheta}\right)' = \Delta L\,,\\ &\left(GJ\vartheta'\right)' - \mu_\vartheta\ddot{\vartheta} - \xi_\vartheta\dot{\vartheta} + x_{CG}\left[m\left(\ddot{\zeta} - x_{CG}\ddot{\vartheta}\right) - \mu_\zeta\left(\ddot{\zeta} - x_{CG}\ddot{\vartheta}\right)'\right] = -\Delta M\,,\end{aligned} \tag{15}$$

which are consistently completed by both geometrical and natural boundary conditions as:

$$\begin{aligned}&\vartheta(0,t) = 0\,, && \zeta(0,t) = 0\,, && \zeta'(0,t) = 0\,,\\ &GJ\vartheta'\big|_l = 0\,, && EIw''\big|_l = 0\,, && \left(EIw''\right)'\big|_l - \bar{T}w'\big|_l - \mu_\zeta\ddot{\zeta}'\big|_l = 0\,,\end{aligned} \tag{16}$$

as well as the initial rest conditions $\zeta(y,0) = 0$, $\dot{\zeta}(y,0) = 0$ and $\vartheta(y,0) = 0$, $\dot{\vartheta}(y,0) = 0$.

3.1 Modal Solution Approach

The Ritz's method is employed and the beam displacement is then modally expressed as:

$$\zeta = \sum_{i=1}^{n_\zeta}\phi_i\varepsilon_i\,, \qquad \vartheta = \sum_{i=1}^{n_\vartheta}\varphi_i\eta_i\,, \qquad \delta\zeta = \sum_{i=1}^{n_\zeta}\phi_i\delta\varepsilon_i\,, \qquad \delta\vartheta = \sum_{i=1}^{n_\vartheta}\varphi_i\delta\eta_i\,, \tag{17}$$

where the n_ζ functions $\varepsilon_i(t)$ and n_ϑ functions $\eta_i(t)$ are unknown generalised coordinates relative to the n_ζ assumed mode shapes $\phi_i(y)$ for bending deformation and n_ϑ assumed mode shapes $\varphi_i(y)$ for torsion deformation, respectively, which are hereby chosen as suitable spanwise polynomials satisfying the geometrical boundary conditions for clamped-free beam [31,33], namely:

$$\phi_i = \left(\frac{y}{l}\right)^{i+1}, \qquad \varphi_i = \left(\frac{y}{l}\right)^{i}, \qquad i \geq 1\,. \tag{18}$$

Note that $\vartheta = -w^*$ and the first assumed torsion mode of the beam model is not allowed by the plate model, due to clamping of the wing root along the entire chord $-b \leq x \leq +b$; yet, its linear behavior can still be recovered by higher assumed torsion modes in a Taylor sense [41].

3.2 Generalised Aerodynamic Load

MST is still employed for calculating the generalised unsteady aerodynamic load. The non-circulatory aerodynamic force and moment of each wing section act at its mid chord (MC), whereas the circulatory ones act at its aerodynamic centre (AC, where the pitching moment is independent of the angle of attack [38-39]) and control point (CP, where the non-penetration boundary condition for the flow is imposed and the fluid-structure interaction [40] hence enforced [38-39]). According to thin aerofoil theory for incompressible flow, aerodynamic centre $x_{AC}(y)$ and control point $x_{CP}(y)$ fall at the first and last quarters of the section chord [19], respectively. The generalised unsteady airload is then implicitly given by:

$$F_i^{\zeta} = \int_0^l \Delta L \phi_i dy\,, \qquad F_i^{\vartheta} = \int_0^l \Delta M \varphi_i dy\,, \tag{19}$$

where the sectional aerodynamic force and pitching moment at the elastic axis read:

$$\Delta L = \kappa\left(\Delta L_W + \Delta L_G\right), \qquad \Delta M = \kappa\left(\Delta M_W + \Delta M_G\right). \tag{20}$$

The airload contributions $\Delta L_W(y,t)$ and $\Delta M_W(y,t)$ due to the wing motion are given by [32,34]:

$$\begin{aligned}
\Delta L_W &= \frac{1}{2}\rho c\left[\frac{\pi c}{2}\left(U\dot{\vartheta} - \ddot{w}_{MC}\right) + UC_{L/\alpha}\left(V_0 \mathrm{W} + \int_0^t \frac{dV(\iota)}{d\iota}\mathrm{W}(t-\iota)d\iota\right)\right], \\
\Delta M_W &= -\frac{1}{2}\rho c\left[\frac{\pi c}{2}\left(\frac{c^2}{32}\ddot{\vartheta} + x_{CP}U\dot{\vartheta} - x_{MC}\ddot{w}_{MC}\right) + x_{AC}UC_{L/\alpha}\left(V_0 \mathrm{W} + \int_0^t \frac{dV(\iota)}{d\iota}\mathrm{W}(t-\iota)d\iota\right)\right],
\end{aligned} \tag{21}$$

where $w_{AC} = \zeta - x_{AC}\vartheta$, $w_{MC} = \zeta - x_{MC}\vartheta$ and $w_{CP} = \zeta - x_{CP}\vartheta$ are instantaneous vertical displacements of the relative section points, whereas $\mathrm{W}(t)$ is the equivalent of Wagner's indicial-admittance function for the circulatory lift build-up due to a unit step in the angle of attack (see Appendix B). Each wing section sees an effective angle of attack induced by the vertical flow velocity $V(y,t)$ due to the instantaneous motion of its control point, namely [32,34]:

$$V = U\vartheta - \dot{w}_{CP}\,, \tag{22}$$

where $V_0 = V(y,0)$ depends on the initial rest conditions; finally, within a "frozen" approach, the additional contributions $\Delta L_G(y,t)$ and $\Delta M_G(y,t)$ due to a vertical wind gust read [32,34]:

$$\Delta L_G = \frac{\Omega}{2}\rho U c C_{L/\alpha}\left(V_{G0}\mathrm{K} + \int_0^t \frac{dV_G(\iota)}{d\iota}\mathrm{K}(t-\iota)d\iota\right), \qquad \Delta M_G = -x_{AC}\Delta L_G\,. \tag{23}$$

As direct analytical cross-validation, Peters' theory is readily recovered by considering its first two chordwise modes only and assuming the lift-curve slope $C_{L/\alpha} = 2\pi$ for a flat airfoil, which is appropriate for a plate wing. Finally, the wing lift, pitching moment and rolling moment are given by [18]:

$$L = \int_0^l \Delta L dy\,, \qquad M_p = \int_0^l \Delta M dy\,, \qquad M_r = \int_0^l y\Delta L dy\,. \tag{24}$$

4 ADDED AERODYNAMIC STATES

For two-dimensional unsteady incompressible potential flow, Theodorsen and Sears [26-28] lift-deficiency functions account for the inflow [19] generated by the travelling wake of a flat aerofoil due an harmonic oscillation and a sinusoidal gust, respectively; the relative indicial-admittance functions for the circulatory lift build-up due to a unit step in the angle of attack and a unit sharp-edge gust are then given by Wagner and Kussner [23-25], respectively.

For three-dimensional flow, all these fundamental functions [44-47] are modified so to include the unsteady downwash of the trailed wing-tip vortices [48-52] and the results are then approximated for computational convenience [53-66]; Appendix B reports the applications to elliptical and trapezoidal wings [20-21]. Due to rigorous analytical continuation [41], with s the Laplace variable, a rational approximation [22,67] is suitably adopted for the equivalent of Theodorsen function in the complex reduced frequency p domain, namely:

$$\mathrm{C} \approx 1 - \frac{A_1^C p}{p + B_1^C} - \frac{A_2^C p}{p + B_2^C}, \qquad p = \frac{sb}{U}, \tag{25}$$

where the coefficients are obtained by best-fitting the analytical reference curve for the specific wing shape, with $A_1^C + A_2^C = 1 - \hat{\mathrm{C}}$ and $\hat{\mathrm{C}} = \lim_{\mathrm{k}\to\infty} \mathrm{C}$ due to exact curve-fitting constraints [68-70]. Being $V = v_0 + \frac{v_1}{2}$ [19], an added aerodynamic state $\upsilon_C(y,t)$ is introduced [71-72] which, due to linearity of the Laplace transform and its inverse [41], evolves from the initial rest condition $\upsilon_C(y,0) = 0$ and $\dot{\upsilon}_C(y,0) = 0$ according to the linear ordinary differential equation (ODE):

$$\ddot{\upsilon}_C + \left(B_1^C + B_2^C\right)\left(\frac{U}{b}\right)\dot{\upsilon}_C + B_1^C B_2^C \left(\frac{U}{b}\right)^2 \upsilon_C = v_0 + \frac{v_1}{2}. \tag{26}$$

Analogously, the equivalent of Wagner function is suitably approximated with two exponential terms [22,67] in the reduced time τ domain, namely:

$$\mathrm{W} = 1 - A_1^W e^{-B_1^W \tau} - A_2^W e^{-B_2^W \tau}, \qquad \tau = \frac{Ut}{b}, \tag{27}$$

where the coefficients are still obtained by best-fitting the analytical reference curve for the specific wing shape, with $A_1^W + A_2^W = 1 - \hat{\mathrm{W}}$ and $\hat{\mathrm{W}} = \lim_{\tau\to 0} \mathrm{W}$ due to exact curve-fitting constraints [68-70]. Another added aerodynamic state $\upsilon_W(y,t)$ is then introduced which evolves from the initial rest condition $\upsilon_W(y,0) = 0$ and $\dot{\upsilon}_W(y,0) = 0$ according to the linear ODE:

$$\ddot{\upsilon}_W + \left(B_1^W + B_2^W\right)\left(\frac{U}{b}\right)\dot{\upsilon}_W + B_1^W B_2^W \left(\frac{U}{b}\right)^2 \upsilon_W = V; \tag{28}$$

of course, note that $A_1^W = A_1^C$, $A_2^W = A_2^C$ and $\hat{\mathrm{W}} = \hat{\mathrm{C}}$ due to reciprocal relations [73-75].

Finally, the equivalent of Kussner function is consistently approximated with two exponential terms [22,67] in the reduced time domain too, namely:

$$\mathrm{K} \approx 1 - A_1^K e^{-B_1^K \tau} - A_2^K e^{-B_2^K \tau}, \tag{29}$$

where the coefficients are obtained by best-fitting the analytical reference curve for the specific wing shape, with $A_1^K + A_2^K = 1$ due to exact curve-fitting constraints [68-70]. So, a further added aerodynamic state $\upsilon_G = \upsilon_G(t)$ is introduced which evolves from the initial rest condition $\upsilon_G(0) = 0$ and $\dot{\upsilon}_G(0) = 0$ according to the linear ODE:

$$\ddot{\upsilon}_G + \left(B_1^K + B_2^K\right)\left(\frac{U}{b}\right)\dot{\upsilon}_G + B_1^K B_2^K \left(\frac{U}{b}\right)^2 \upsilon_G = V_G; \tag{30}$$

note that this equation is uncoupled from all others and hence does not affect the aeroelastic stability of the wing, in the present framework of a linear model for small perturbations [10].

4.1 Plate Model

The unsteady generalised aerodynamic load per unit span is eventually given by:

$$\begin{aligned}
\Delta F_0^a &= -\pi\rho b^2\left(\ddot{w}_0 - \frac{\ddot{w}_2}{2}\right) - 2\pi\rho bU\left[\hat{\mathrm{C}}\dot{w}_0 + \left(\frac{1+\hat{\mathrm{C}}}{2}\right)\dot{w}_1\right] - 2\pi\rho U^2\hat{\mathrm{C}}\sum_{k=1}^{n_k} k w_k + \\
&+ 2\pi\rho bU\left[\left(A_1^C B_1^C + A_2^C B_2^C\right)\left(\frac{U}{b}\right)\dot{\upsilon}_C + \left(1-\hat{\mathrm{C}}\right)B_1^C B_2^C\left(\frac{U}{b}\right)^2\upsilon_C\right] + \Delta F_0^G, \\
\Delta F_1^a &= -\frac{\pi}{8}\rho b^2\left(\ddot{w}_1 - \ddot{w}_3\right) + \pi\rho bU\left[\hat{\mathrm{C}}\dot{w}_0 - \left(\frac{1-\hat{\mathrm{C}}}{2}\right)\dot{w}_1 - \dot{w}_2\right] + \pi\rho U^2\left[\hat{\mathrm{C}}w_1 - \left(1-\hat{\mathrm{C}}\right)\sum_{k=2}^{n_k} k w_k\right] + \\
&- \pi\rho bU\left[\left(A_1^C B_1^C + A_2^C B_2^C\right)\left(\frac{U}{b}\right)\dot{\upsilon}_C + \left(1-\hat{\mathrm{C}}\right)B_1^C B_2^C\left(\frac{U}{b}\right)^2\upsilon_C\right] + \Delta F_1^G, \\
\Delta F_2^a &= \frac{\pi}{2}\rho b^2\left(\ddot{w}_0 - \frac{2}{3}\ddot{w}_2 + \frac{\ddot{w}_4}{6}\right) + \pi\rho bU\left(\dot{w}_1 - \dot{w}_3\right) + 2\pi\rho U^2 w_2, \\
\Delta F_k^a &= \frac{\pi}{4}\rho b^2\left[\frac{1}{k-1}\left(\ddot{w}_{k-2} - \ddot{w}_k\right) - \frac{1}{k+1}\left(\ddot{w}_k - \ddot{w}_{k+2}\right)\right] + \pi\rho bU\left(\dot{w}_{k-1} - \dot{w}_{k+1}\right) + \pi\rho U^2 k w_k,
\end{aligned} \tag{31}$$

the incremental contribution due to gust being:

$$\begin{aligned}
\Delta F_0^G &= 2\pi\rho bU\Omega\left[\left(A_1^K B_1^K + A_2^K B_2^K\right)\left(\frac{U}{b}\right)\dot{\upsilon}_G + B_1^K B_2^K\left(\frac{U}{b}\right)^2\upsilon_G\right], \\
\Delta F_1^G &= -\pi\rho bU\Omega\left[\left(A_1^K B_1^K + A_2^K B_2^K\right)\left(\frac{U}{b}\right)\dot{\upsilon}_G + B_1^K B_2^K\left(\frac{U}{b}\right)^2\upsilon_G\right],
\end{aligned} \tag{32}$$

and the linear ODE for added aerodynamic state evolution reading:

$$\ddot{\upsilon}_C + \left(B_1^C + B_2^C\right)\left(\frac{U}{b}\right)\dot{\upsilon}_C + B_1^C B_2^C\left(\frac{U}{b}\right)^2 \upsilon_C = -\dot{w}_0 - \frac{\dot{w}_1}{2} - \frac{U}{b}\sum_{k=1}^{n_k} k w_k \ . \tag{33}$$

Thus, by expanding $\upsilon_C = \sum_{j=1}^{n_j} f_j \upsilon_j$ and $\Delta F_k^a = \sum_{j=1}^{n_j} f_j \Delta F_j^k + \Delta F_k^G$ in a consistent way, the unsteady sectional airload is eventually expressed in terms of the generalised coordinates ε_i. In essence, each term of Peters' theory (added states included) is projected onto the assumed spanwise modes f_j and the generalised aerodynamic matrices are then assembled by blocks.

4.2 Beam Model

The unsteady generalised aerodynamic load per unit span due to the wing motion is eventually given by:

$$\begin{aligned}
\Delta L_W &= \frac{\pi}{4}\rho c^2\left(U\dot{\vartheta} - \ddot{\zeta} + x_{MC}\ddot{\vartheta}\right) + \frac{\hat{\mathrm{W}}}{2}\rho U c C_{L/\alpha}\left(U\vartheta - \dot{\zeta} + x_{CP}\dot{\vartheta}\right) + \\
&+ \frac{1}{2}\rho U c C_{L/\alpha}\left[\left(A_1^W B_1^W + A_2^W B_2^W\right)\left(\frac{U}{b}\right)\left(\dot{\upsilon}_\zeta + \dot{\upsilon}_\vartheta\right) + \left(A_1^W + A_2^W\right)B_1^W B_2^W\left(\frac{U}{b}\right)^2\left(\upsilon_\zeta + \upsilon_\vartheta\right)\right], \\
\Delta M_W &= -\frac{\pi}{4}\rho c^2\left[\frac{c^2}{32}\ddot{\vartheta} + x_{CP}U\dot{\vartheta} - x_{MC}\left(\ddot{\zeta} - x_{MC}\ddot{\vartheta}\right)\right] - \frac{\hat{\mathrm{W}}}{2}\rho U x_{AC} c C_{L/\alpha}\left(U\vartheta - \dot{\zeta} + x_{CP}\dot{\vartheta}\right) + \\
&- \frac{1}{2}\rho U x_{AC} c C_{L/\alpha}\left[\left(A_1^W B_1^W + A_2^W B_2^W\right)\left(\frac{U}{b}\right)\left(\dot{\upsilon}_\zeta + \dot{\upsilon}_\vartheta\right) + \left(A_1^W + A_2^W\right)B_1^W B_2^W\left(\frac{U}{b}\right)^2\left(\upsilon_\zeta + \upsilon_\vartheta\right)\right],
\end{aligned} \tag{34}$$

the incremental contribution due to gust being:

$$\Delta L_G = \frac{1}{2}\rho U c C_{L/\alpha}\left[\left(A_1^K B_1^K + A_2^K B_2^K\right)\left(\frac{U}{b}\right)\dot{\upsilon}_G + \left(A_1^K + A_2^K\right)B_1^K B_2^K\left(\frac{U}{b}\right)^2 \upsilon_G\right], \tag{35}$$

where, with $\upsilon_W = \upsilon_\zeta + \upsilon_\vartheta$ due to linearity, the added aerodynamic states $\upsilon_\zeta(y,t)$ and $\upsilon_\vartheta(y,t)$ are relative to the wing bending and torsion motion and evolve from their initial rest condition $\upsilon_\zeta(y,0) = 0$, $\upsilon_\vartheta(y,0) = 0$ and $\dot{\upsilon}_\zeta(y,0) = 0$, $\dot{\upsilon}_\vartheta(y,0) = 0$ according to the linear ODEs:

$$\begin{aligned}
\ddot{\upsilon}_\zeta + \left(B_1^W + B_2^W\right)\left(\frac{U}{b}\right)\dot{\upsilon}_\zeta + B_1^W B_2^W\left(\frac{U}{b}\right)^2 \upsilon_\zeta &= -\ddot{\zeta}\ , \\
\ddot{\upsilon}_\vartheta + \left(B_1^W + B_2^W\right)\left(\frac{U}{b}\right)\dot{\upsilon}_\vartheta + B_1^W B_2^W\left(\frac{U}{b}\right)^2 \upsilon_\vartheta &= U\vartheta + x_{CP}\dot{\vartheta}\ .
\end{aligned} \tag{36}$$

As $\Delta L_W = \Delta L_\zeta + \Delta L_\vartheta$ and $\Delta M_W = \Delta M_\zeta + \Delta M_\vartheta$ due to assumed linearity, by expanding $\Delta L_\zeta = \sum_{i=1}^{n_\zeta} \phi_i \Delta L_i^\zeta$, $\Delta L_\vartheta = \sum_{i=1}^{n_\vartheta} \varphi_i \Delta L_i^\vartheta$ and $\Delta M_\zeta = \sum_{i=1}^{n_\zeta} \phi_i \Delta M_i^\zeta$, $\Delta M_\vartheta = \sum_{i=1}^{n_\vartheta} \varphi_i \Delta M_i^\vartheta$ as well as $\upsilon_\zeta = \sum_{i=1}^{n_\zeta} \phi_i \upsilon_i^\zeta$ and $\upsilon_\vartheta = \sum_{i=1}^{n_\vartheta} \varphi_i \upsilon_i^\vartheta$ in a consistent way, the unsteady sectional airload is finally expressed in terms of the generalised coordinates ε_i and η_i. In essence, each term of strip theory (added states included) is projected onto the assumed spanwise modes ϕ_i and φ_i, respectively, and the generalised aerodynamic matrices are then assembled by blocks.

5 MODIFIED STRIP THEORY

Within the framework of TST and MST [14-16], the scaling function $\kappa(y)$ accounts for the three-dimensional spanwise influence of the wing-tip vortices on the sectional airload and is consistently derived from Kutta-Joukowsky's theorem [76-77] as:

$$\kappa_{TST} = \frac{\pi AR}{\pi AR + C_{L/\alpha}}, \qquad \kappa_{MST} = \frac{2\Gamma}{UcC_{L/\alpha}}, \qquad \Gamma = lU \sum_{q=1}^{n_\Gamma} \Gamma_q \sin(q\psi), \tag{37}$$

where the sectional flow circulation $\Gamma(y)$ is directly related to the downwash angle by Helmholtz's theorem and Biot-Savart law [17] and is explicitly given by Prandtl's expansion [78], with the n_Γ coefficients Γ_q found by solving the linear system of algebraic equations:

$$\sum_{q=1}^{n_\Gamma} \left(\sin(q\psi) + q \frac{cC_{L/\alpha}}{8l} \frac{\sin(q\psi)}{\sin\psi} \right) \Gamma_q = \frac{cC_{L/\alpha}}{2l}, \tag{38}$$

in a least-squares sense [79], on N wing sections at various spanwise stations $y = l\cos(\psi)$, with $0 \le \psi \le \pi$ running from tip to tip along the span. Note that $\Gamma = 0$ for $c = 0$, while the singularities at $\psi = j\pi$ can be lifted by multiplying both sides of the equation by $\sin\psi$. Also note that odd and even Fourier terms model symmetric and antisymmetric circulation distributions, respectively.

Essentially, within TST the airflow around each wing section is still considered fully independent and two-dimensional: a global scaling factor is applied to the wing lift and standard strip theory (SST, where any three-dimensional effect is disregarded [18]) is indeed obtained for the limit of infinitely long wing (Theodorsen/Wagner and Sears/Kussner functions shall hence coherently be employed as lift-deficiency functions). On the contrary, within MST the airflow around each wing section is considered quasi-independent and a unitary angle of attack is implicitly assumed for calculating the scaling function without loss of generality. In both cases, the correction is based on the undeformed wing [80] and rigorously valid in the low-subsonic regime for thin straight wings with significant aspect ratio.

Finally, it is also worth stressing that κ is here based on lifting line theory (LLT, of which SST is the forcing term [78]) and MST may then be regarded as a simplified quasi-steady realisation of unsteady LLT [81-83] but the overall tuning concept is completely general [84-87]

and such function may then be derived based on the circulation distribution obtained from any other appropriate source, such as VLM [17], DLM [88-89], CFD [90] or experimental data. In the case of non-planar wings [91-92], the scaling function would also include the geometrically nonlinear effects of the wing curvature on the local loads [93].

6 AEROELASTIC RESPONSE AND STABILITY ANALYSIS

By substituting the modal expansions in the PVW, the aeroelastic equilibrium PDE eventually becomes a linear system of ODEs for the generalised coordinates regardless the aero-structural model, namely [94]:

$$\mathbf{M}^{\mathbf{s}}\ddot{\boldsymbol{\chi}}+\mathbf{C}^{\mathbf{s}}\dot{\boldsymbol{\chi}}+\mathbf{K}^{\mathbf{s}}\boldsymbol{\chi}=\mathbf{F}^{\mathbf{a}}, \qquad \mathbf{F}^{\mathbf{a}}=\mathbf{M}^{\mathbf{a}}\ddot{\boldsymbol{\chi}}+\mathbf{C}^{\mathbf{a}}\dot{\boldsymbol{\chi}}+\mathbf{K}^{\mathbf{a}}\boldsymbol{\chi}+\mathbf{F}^{\mathbf{G}}, \tag{39}$$

with the initial rest condition $\boldsymbol{\varepsilon}(0)=\mathbf{0}$ and $\dot{\boldsymbol{\varepsilon}}(0)=\mathbf{0}$, where the generalised structural mass $\mathbf{M}^{\mathbf{s}}$, damping $\mathbf{C}^{\mathbf{s}}$ and stiffness $\mathbf{K}^{\mathbf{s}}$ matrices are given in Appendix A, whereas the generalised aerodynamic load vector $\mathbf{F}^{\mathbf{a}}(t)$ as well as generalised aerodynamic mass $\mathbf{M}^{\mathbf{a}}$, damping $\mathbf{C}^{\mathbf{a}}$ and stiffness $\mathbf{K}^{\mathbf{a}}$ matrices and generalised gust load vector $\mathbf{F}^{\mathbf{G}}(t)$ depend on the wing shape; $\boldsymbol{\chi}(t)$ is the vector of all unknown generalised coordinates (including added aerodynamic states) and drives the aeroelastic dynamic response. Note that a change of variables is always possible as long as a proper transformation matrix can be defined and all aero-structural matrices are then consistently projected onto the new modal base [10,19].

The aeroelastic behaviour and stability analysis of the subsonic wing are then governed by:

$$\mathbf{M}\ddot{\boldsymbol{\chi}}+\mathbf{C}\dot{\boldsymbol{\chi}}+\mathbf{K}\boldsymbol{\chi}=\mathbf{F}^{\mathbf{G}}, \qquad \det\left(\mathbf{M}\lambda^2+\mathbf{C}\lambda+\mathbf{K}\right)=0, \tag{40}$$

respectively, or their equivalent first-order forms [94]:

$$\begin{Bmatrix}\ddot{\boldsymbol{\chi}}\\ \dot{\boldsymbol{\chi}}\end{Bmatrix}=\begin{bmatrix}-\mathbf{M}^{-1}\mathbf{C} & -\mathbf{M}^{-1}\mathbf{K}\\ \mathbf{I} & \mathbf{0}\end{bmatrix}\begin{Bmatrix}\dot{\boldsymbol{\chi}}\\ \boldsymbol{\chi}\end{Bmatrix}+\begin{Bmatrix}\mathbf{M}^{-1}\mathbf{F}^{\mathbf{G}}\\ \mathbf{0}\end{Bmatrix}, \qquad \det\begin{bmatrix}\mathbf{I}\lambda+\mathbf{M}^{-1}\mathbf{C} & \mathbf{M}^{-1}\mathbf{K}\\ -\mathbf{I} & \mathbf{I}\lambda\end{bmatrix}=0, \tag{41}$$

where $\mathbf{M}=\mathbf{M}^{\mathbf{s}}-\mathbf{M}^{\mathbf{a}}$, $\mathbf{C}=\mathbf{C}^{\mathbf{s}}-\mathbf{C}^{\mathbf{a}}$ and $\mathbf{K}=\mathbf{K}^{\mathbf{s}}-\mathbf{K}^{\mathbf{a}}$ are the generalised aeroelastic mass, damping and stiffness matrices, which depend parametrically on the flow speed. In particular, flutter occurs at the lowest flow speed U_F which makes the real part of at least one of the complex eigenvalues λ_i become positive (i.e., the dynamic behaviour becomes unstable thru a Hopf bifurcation [35], where a couple of complex conjugates eigenvalues crosses the imaginary axis and leaves the response undamped), two or even more generalised aeroelastic modes coupling at the flutter frequency f_F. Note that real and imaginary parts of the complex eigenvalue are related to the effective damping and vibration frequency of the wing, respectively, its natural vibration modes being correctly recovered in the absence of airflow [43]. The static divergence speed, instead, is the lowest flow speed U_D which makes at least one of the complex eigenvalues cross the imaginary axis along the real axis, the aeroelastic stiffness matrix becoming singular (i.e., structural and aerodynamic forces do not find a stable equilibrium) for steady flow [35].

7 RESULTS AND DISCUSSION

A flat rectangular wing of uniform material is considered; due to clamping at the root, it is:

$$EI_x = EI_y = \frac{Eh^3}{12\left(1-\nu^2\right)}, \qquad EI_{xy} = EI_{yx} = \frac{\nu Eh^3}{12\left(1-\nu^2\right)}, \qquad GJ_{xy} = \frac{Eh^3}{6\left(1+\nu\right)}\left(1-\frac{3h}{5c}\right), \tag{42}$$

for the rectangular cross-section of the plate-like structural model [29-30,95], while the second moments of inertia per unit area read:

$$\mu_x = \frac{mh^2}{12}, \qquad \mu_y = \frac{m}{12}\left(h^2+c^2\right), \tag{43}$$

being $EI = cEI_y$ and $GJ = cGJ_{xy}$ as well as $\mu_\zeta = c\mu_x$ and $\mu_\vartheta = c\mu_y$ for the beam-like structural model [31-32,95]; in both cases, elastic and inertial axes coincide with the symmetry $\hat{\mathbf{y}}$ axis. The developed code is then validated with respect to a previous fundamental work [96], where the wing geometry is defined by $l = 0.305\,\text{m}$, $c = 0.0762\,\text{m}$ and $h = 0.00044\,\text{m}$ (i.e., $AR \approx 8$ and $TR \approx 0.006$) and an elastic material with $\rho_s = 2768\,\text{kg/m}^3$, $E = 74^9\,\text{Pa}$ and $\nu = 0.33$ is assumed; pretension and structural damping are neglected. By coupling a plate-like finite elements (FE) structural model [97] with a DLM [98] aerodynamic model via spline interface [99] for transferring loads and displacements, a flutter speed $U_F = 20.61\,\text{m/s}$ was numerically obtained with the *p-k* method [100] and a non-iterative frequency sweeping technique [101], where the first ten eigenmodes were considered and mode-tracking was performed via eigenvectors correlation matrix [102]. The proposed semi-analytical plate-like model with LLT scaling function detects the flutter instability at $U_F = 20.2\,\text{m/s}$, in excellent agreement with the literature results. The first three spanwise and chordwise assumed structural modes along with the first ten LLT aerodynamic modes granted convergence; the coefficients for the lift-deficiency function due to a unit step in angle of attack are shown in Table 1, whereas the indicial function itself is shown in Figure 1 along with the LLT scaling function. Similar conclusions can coherently be drawn when the elastic material is assumed with $\rho_s = 2800\,\text{kg/m}^3$ and $E = 103^9\,\text{Pa}$, as a flutter speed $U_F = 24.78\,\text{m/s}$ was found in the literature, while the proposed model detects the flutter instability at $U_F = 24.3\,\text{m/s}$, still in remarkable agreement.

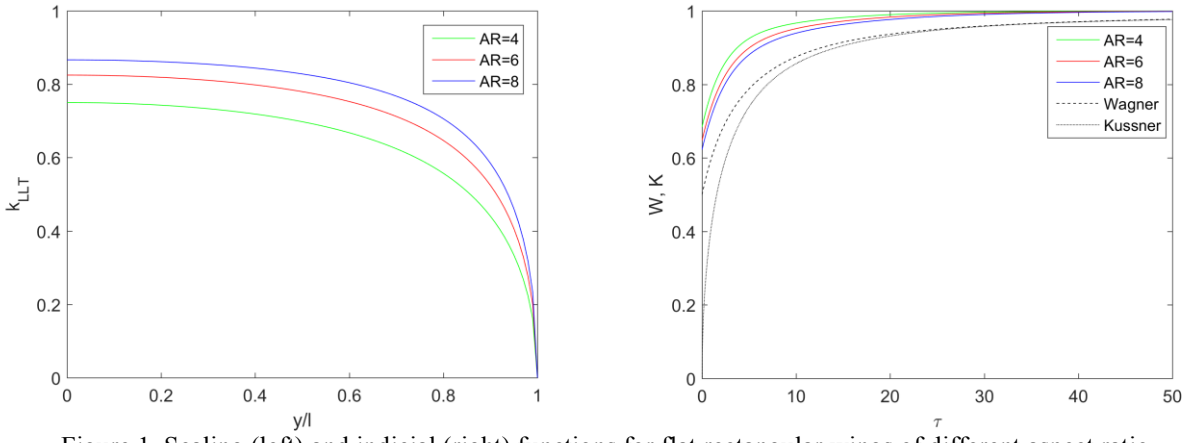

Figure 1. Scaling (left) and indicial (right) functions for flat rectangular wings of different aspect ratio.

AR	4	5	6	7	8	∞
e	0.120	0.141	0.161	0.179	0.195	—
$A_1^W \equiv A_1^C$	0.114	0.130	0.142	0.151	0.159	0.165
$A_2^W \equiv A_2^C$	0.265	0.272	0.276	0.278	0.279	0.335
$B_1^W \equiv B_1^C$	0.111	0.104	0.098	0.093	0.088	0.045
$B_2^W \equiv B_2^C$	0.473	0.445	0.428	0.416	0.407	0.300
$\hat{W} \equiv \hat{C}$	0.621	0.598	0.582	0.571	0.562	0.500

Table 1. Coefficients for the lift-deficiency function due to a unit step in angle of attack.

Neglecting pretension and structural damping without loos of generality, divergence speed, flutter speed and flutter frequency are then investigated with respect to both aspect and thickness ratios for a uniform wing with $\rho_s = 2700\,\mathrm{kg/m^3}$, $E = 70^9\,\mathrm{Pa}$ and $\nu = 0.35$. Figures 2 to 4 show the numerical results obtained with either TST (left) or MST (right); in the latter case, perfect agreement was found with the exact analytical results for the divergence speed of the beam-like wing model, thus providing with direct validation. It is worth stressing that, despite lacking the chordwise degree of freedom [10], the beam-based analysis is more conservative than the plate-based ones, as the first assumed torsion mode of the beam model is formally not allowed by the plate model due to the wing root clamping.

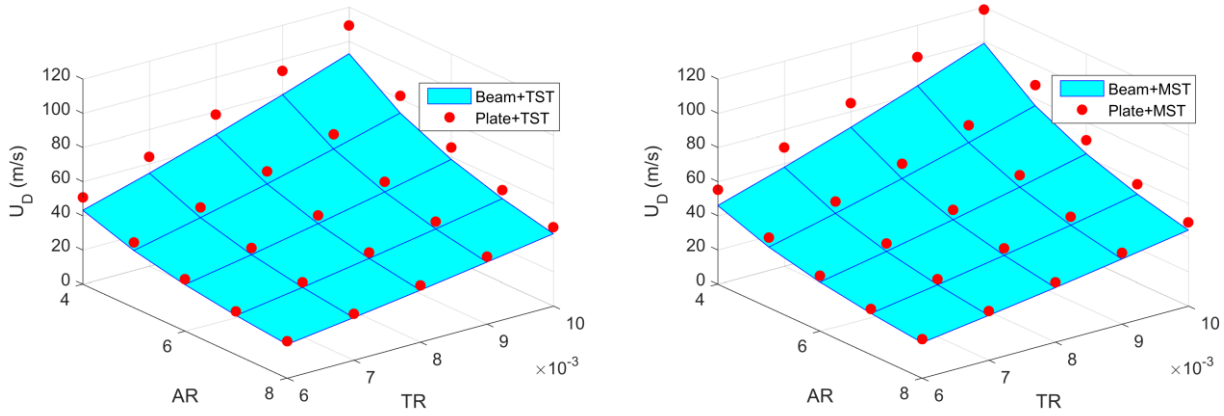

Figure 2. Divergence speed for uniform rectangular wing, according to subsonic TST (left) and MST (right).

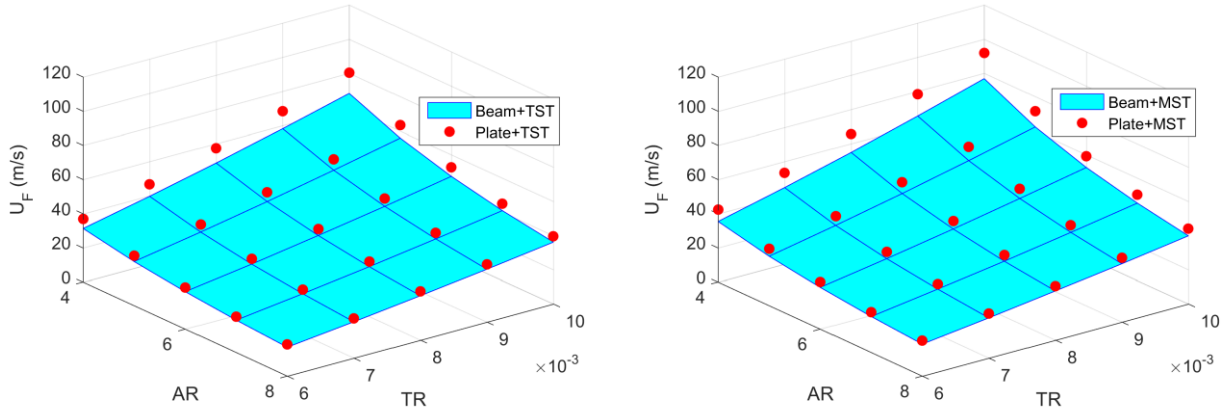

Figure 3. Flutter speed for uniform rectangular wing, according to subsonic TST (left) and MST (right).

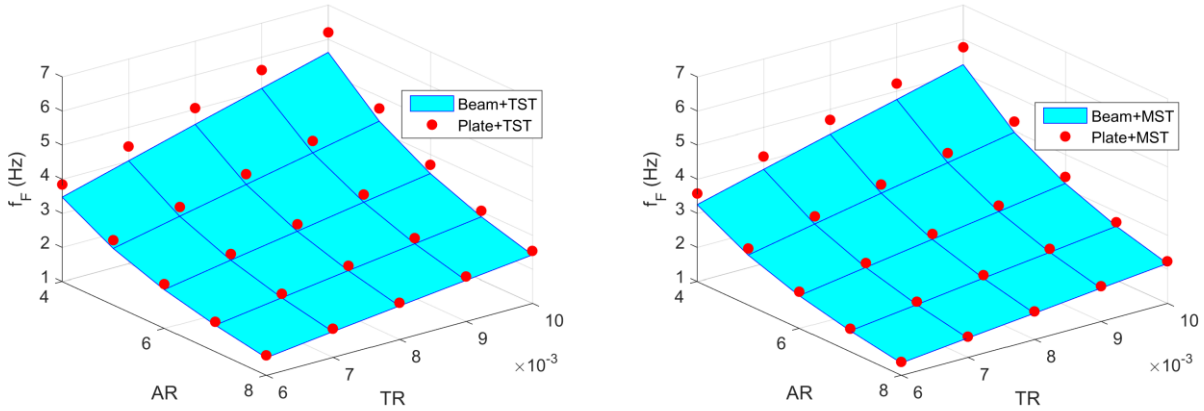

Figure 4. Flutter frequency for uniform rectangular wing, according to subsonic TST (left) and MST (right).

Of course, the TST-based results are more conservative than the MST-based ones, as in the latter case the aerodynamic load decays rapidly towards the wing tip, which is the "weakest" area; indeed, the resulting bending moment at the wing root is lower in the MST-based cases. As expected, the (percentage) difference between plate-based and beam-based results remains roughly constant with varying the thickness ratio, whereas it consistently diminishes with increasing the aspect ratio; due to the three-dimensional downwash effect, the same is true for the relative (percentage) difference between MST-based and TST-based results. Still, the first three spanwise and chordwise assumed structural modes along with the first ten LLT aerodynamic modes granted convergence in all cases; as anticipated, the effect of higher-order camber modes for the plate-like wing could not be appreciated, as the wing root is fully clamped. As further cross-validation, the results difference became fairly negligible when the same aerodynamic model was used and only the first two chordwise modes were considered in the plate-based model while coincident modes were assumed for both bending and torsion in the beam-based model (so that identical boundary conditions were applied at the wing root).

8 CONCLUSION

A computationally efficient semi-analytical model for the combined aeroelastic analysis and dynamic response of flexible subsonic wings has been presented. A new modified strip theory was first formulated for the unsteady aerodynamic load and then coupled with a plate model for the structural behaviour. The principle of virtual works was employed to derive the equilibrium equations, which were finally solved within a modal approach for the wing displacement. Tuned strip theory was also considered, in order to account for three-dimensional flow effects in different ways. Based on a general variational formulation, the proposed aeroelastic models allow any arbitrary distribution of the flexible wing's physical properties and provide with a continuous solution of the wing's displacement along the surface, as suitable for parametric optimisation studies within preliminary wing design. Numerical results were obtained and compared for the divergence speeds and flutter frequency of a flat rectangular wing with constant structural properties, for different values of aspect ratio and thickness ratio. Semi-analytical solutions with a beam model have also been derived for rigorous validation purposes. All presented results provide sound insights on the behaviour of flexible subsonic wings and may be used to assess high-fidelity aeroelastic tools, also in terms of computational efficiency. The modified strip theory showed an excellent compromise between the lower

computational cost and complexity of strip theory and the higher accuracy of unsteady lifting line theory and it is hence suggested as a general and effective aerodynamic tool for the multidisciplinary design and optimisation of flexible subsonic wings, particularly at the preliminary stage where fast semi-analytical aeroelastic simulations are intensively sought.

REFERENCES

[1] E. Livne, The Future of Aircraft Aeroelasticity. *Journal of Aircraft*, **40** (**6**), 2003.

[2] L. Cavagna, et al., NeoCASS: An Integrated Tool for Structural Sizing, Aeroelastic Analysis and MDO at Conceptual Design Level. *Progress in Aerospace Sciences*, **47** (**8**), 2011.

[3] Z.Q. Qu, *Model Order Reduction Techniques with Applications in Finite Element Analysis*. Springer-Verlag, 2004.

[4] A. Quarteroni, G. Rozza, *Reduced Order Methods for Modeling and Computational Reduction*. Springer International Publishing, 2014.

[5] M. Gennaretti, F. Mastroddi, Study of Reduced-Order Models for Gust-Response Analysis of Flexible Fixed Wings. *Journal of Aircraft*, **41** (**2**), 2004.

[6] M. Ghoreyshi, et al., Reduced Order Unsteady Aerodynamic Modeling for Stability and Control Analysis Using Computational Fluid Dynamics. *Progress in Aerospace Sciences*, **71**, 2014.

[7] N.M. Alexandrov, M.Y. Hussaini, *Multidisciplinary Design Optimization: State of the Art*. Proceedings in Applied Mathematics Series, SIAM, 1997.

[8] E. Kesseler, M. Guenov, *Advances in Collaborative Civil Aeronautical Multidisciplinary Design Optimization*. Progress in Astronautics and Aeronautics Series, AIAA, 2010.

[9] M. Berci, et al., Multifidelity Metamodel Building as a Route to Aeroelastic Optimization of Flexible Wings. *Journal of Mechanical Engineering Science (Proceedings of the Institution of Mechanical Engineers - Part C)*, **225** (**9**), 2011.

[10] M. Berci, et al., A Semi-Analytical Model for the Combined Aeroelastic Behaviour and Gust Response of a Flexible Aerofoil. *Journal of Fluids and Structures*, **37**, 2013.

[11] T. Sucipto, et al., Gust Response of a Flexible Typical Section via High- and (Tuned) Low-Fidelity Simulations. *Computers and Structures*, **122**, 2013.

[12] M. Berci, et al., Dynamic Response of Typical Section Using Variable-Fidelity Fluid Dynamics and Gust-Modeling Approaches - With Correction Methods. *Journal of Aerospace Engineering*, **27** (**5**), 2014.

[13] M. Berci, et al., Multidisciplinary Multifidelity Optimisation of a Flexible Wing Aerofoil with Reference to a Small UAV. *Structural and Multidisciplinary Optimization*, **50** (**4**), 2014.

[14] M. Berci, Semi-Analytical Static Aeroelastic Analysis and Response of Flexible Subsonic Wings. *Applied Mathematics and Computations*, **267**, 2015.

[15] F.W. Diederich, Approximate Aerodynamic Influence Coefficients for Wings of Arbitrary Plan Form in Subsonic Flow. NACA TN 2092, 1950.

[16] F.W. Diederich, M. Zlotnick, Calculated Spanwise Lift Distributions, Influence Functions and Influence Coefficients for Unswept Wings in Subsonic Flow. NACA 1228, 1955.

[17] J. Katz, A. Plotkin, *Low Speed Aerodynamics*. Cambridge University Press, 2001.

[18] J.D. Anderson, *Fundamentals of Aerodynamics*. McGraw-Hill, 2007.

[19] D.A. Peters, et al, A State-Space Airloads Theory for Flexible Airfoils. *Journal of the American Helicopter Society*, **52** (**4**), 2007.

[20] R.T. Jones, The Unsteady Lift of a Wing of Finite Aspect Ratio. NACA 681, 1940.

[21] M.J. Queijo, et al., Approximate Indicial Lift Function for Tapered, Swept Wings in Incompressible Flow. NASA TP-1241, 1978.

[22] M. Berci, Semi-Analytical Reduced-Order Models for the Unsteady Aerodynamic Loads of Subsonic Wings. 5th ECCOMAS COMPDYN, Crete, 2015.

[23] H. Wagner, Uber die Entstenhung des Dynamischen Auftriebes von Tragflugeln. *Zeitschrift für Angewandte Mathematik und Mechanik*, **5** (**1**), 1925.

[24] H.G. Kussner, Zusammenfassender Beritch uber den Instationaren Auftrieb von Flugeln. *Luftfahrtforsch*, **13** (**12**), 1936.

[25] A. Kayran, Küssner's Function in the Sharp Edged Gust Problem - A Correction. *Journal of Aircraft*, **43** (**5**), 2006.

[26] T. Theodorsen, General Theory of Aerodynamic Instability and the Mechanism of Flutter. NACA 496, 1935.

[27] T. Von Karman, W.R. Sears, Airfoil Theory for Non-Uniform Motion, *Journal of the Aeronautical Sciences*, **5** (**10**), 1938.

[28] W.R. Sears, Operational Methods in the Theory of Airfoils in Non-Uniform Motion. *Journal of the Franklin Institute*, **230** (**1**), 1940.

[29] R.L. Bisplinghoff, H. Ashley, *Principles of Aeroelasticity*. Dover, 2013.

[30] M. Amabili, *Nonlinear Vibrations and Stability of Shells and Plates*. Cambridge University Press, 2008.

[31] D.H. Hodges, G.A. Pierce, *Introduction to Structural Dynamics and Aeroelasticity*. Cambridge University Press, 2002.

[32] R.L. Bisplinghoff, et al., *Aeroelasticity*. Dover, 1996.

[33] L. Demasi, E. Livne, Structural Ritz-Based Simple-Polynomial Nonlinear Equivalent Approach - An Assessment. AIAA-2005-2093, 2005.

[34] Y.C. Fung, *An Introduction to the Theory of Aeroelasticity*. Dover, 1993.

[35] J.R. Wright, J.E. Cooper, *Introduction to Aircraft Aeroelasticity and Loads*. AIAA Education Series, AIAA, 2007.

[36] B. Yang, *Strain, Stress and Structural Dynamics*. Elsevier, 2005.

[37] H. Glauert, *The Elements of Aerofoil and Airscrew Theory*. Cambridge University Press, 1947.

[38] R.T. Jones, Classical Aerodynamic Theory. NASA RP 1050, 1979.

[39] U. Gulcat, *Fundamentals of Modern Unsteady Aerodynamics*. Springer, 2011.

[40] H.J. Bungartz, M. Schafer, *Fluid-Structure Interaction: Modelling, Simulation, Optimization*. Springer, 2006.

[41] A. Quarteroni, et al., *Numerical Mathematics*. Springer-Verlag, 2000.

[42] F.M. Hoblit, *Gust Loads on Aircraft: Concepts and Applications*. AIAA Education Series, AIAA, 1988.

[43] S.M. Han, et al., Dynamics of Transversally Vibrating Beams Using Four Engineering Theories. *Journal of Sound and Vibration*, **225** (**5**), 1999.

[44] M. Tobak, On the Use of the Indicial-Function Concept in the Analysis of Unsteady Motions of Wings and Wing-Tail Combinations. NACA 1188, 1954.

[45] E.C. Pike, Manual on Aeroelasticity. AGARD 578, 1971.

[46] W. Silva, Discrete-Time Linear and Nonlinear Aerodynamic Impulse Responses for Efficient Use of CFD Analyses. *PhD Thesis*, College of William & Mary, 1997.

[47] M. Ghoreyshi, et al., Computational Investigation into the Use of Response Functions for Aerodynamic-Load Modeling. *AIAA Journal*, **50** (**6**), 2012.

[48] W.P. Jones, Aerodynamic Forces on Wings in Simple Harmonic Motion. ARC-RM-2026, 1945.

[49] W.P. Jones, Aerodynamic Forces on Wings in Non-Uniform Motion. ARC-RM-2117, 1945.

[50] E. Reissner, Effect of Finite Span on the Airload Distributions for Oscillating Wings – Part I: Aerodynamic Theory of Oscillating Wings of Finite Span. NACA TN-1194, 1947.

[51] E. Reissner, J.E. Stevens, Effect of Finite Span on the Airload Distributions for Oscillating Wings – Part II: Methods of Calculation and Examples of Application. NACA TN-1194, 1947.

[52] J.A. Drischler, Approximate Indicial Lift Function for Several Wings of Finite Span in Incompressible Flow as obtained from Oscillatory Lift Coefficients. NACA TN-3639, 1956.

[53] R. Vepa, On the Use of Padè Approximants to Represent Unsteady Aerodynamic Loads for Arbitrarily Small Motions of Wings. AIAA-76-17, 1976.

[54] R. Vepa, Finite State Modeling of Aeroelastic System. NASA-CR-2779, 1977.

[55] K.L. Roger, Airplane Math Modeling Methods for Active Control Design. AGARD-CP-228, 1977.

[56] R.N. Desmarais, A Continued Fraction Representation for Theodorsen's Circulation Function. NASA-TM-81838, 1980.

[57] E.H. Dowell, A Simple Method for Converting Frequency Domain Aerodynamics to the Time Domain. NASA-TM-81844, 1980.

[58] H. Dunn, An Analytical Technique for Approximating Unsteady Aerodynamics in the Time Domain. NASA-TP-1738, 1980.

[59] T.S. Beddoes, Practical Computation of Unsteady Lift. *Vertica*, **8** (**1**), 1984.

[60] C. Venkatesan, P. Friedmann, New Approach to Finite-State Modeling of Unsteady Aerodynamics. *AIAA Journal*, **24** (**12**), 1986.

[61] L.D. Peterson, E.F. Crawley, Improved Exponential Time Series Approximations of Unsteady Aerodynamic Operators. *Journal of Aircraft*, **25** (**2**), 1988.

[62] W. Eversman, A. Tewari, Modified Exponential Series Approximation for the Theodorsen Function. *Journal of Aircraft*, **28** (**9**), 1991.

[63] A. Tewari, J. Brink-Spalink, Multiple Pole Rational-Function Approximations for Unsteady Aerodynamics. *Journal of Aircraft*, **30** (**3**), 1993.

[64] M. Karpel, E. Strul, Minimum-State Unsteady Aerodynamic Approximations with Flexible Constraints, *Journal of Aircraft*, **33** (**6**), 1996.

[65] I. Cotoi, R.M. Botez, Method of Unsteady Aerodynamic Forces Approximation for Aeroservoelastic Interactions. *Journal of Guidance, Control and Dynamics*, **25** (**5**), 2002.

[66] S.L. Brunton, C.W. Rowley, Empirical State-Space Representations for Theodorsen's Lift Model. *Journal of Fluids and Structures*, **38** (**1**), 2013.

[67] J.G. Leishman, *Principles of Helicopter Aerodynamics*. Cambridge Aerospace Series, Cambridge University Press, 2006.

[68] R.B. Holmes, *A Course on Optimization and Best Approximation*. Lecture Notes in Mathematics, Springer, 1972.

[69] S.H. Tiffany, W.M. Adams, Nonlinear Programming Extensions to Rational Function Approximation Methods for Unsteady Aerodynamic Forces. NASA-TP-2776, 1988.

[70] M. Berci, Optimal Approximations of Indicial Aerodynamics. *Proceedings of the 1st OPTi*, 2014.

[71] J.G. Leishman, K.Q. Nguyen, State-Space Representation of Unsteady Airfoil Behavior. *AIAA Journal*, **28** (**5**), 1990.

[72] M. Meyer, H.G. Matthies, State-Space Representation of Instationary Two-Dimensional Airfoil Aerodynamics. *Journal of Wind Engineering and Industrial Aerodynamics*, **92** (**3-4**), 2004.

[73] L.E. Garrick, On some Reciprocal Relations in the Theory of Nonstationary Flows. NACA-629, 1938.

[74] M.A. Heaslet, J.R. Spreiter, Reciprocity Relations in Aerodynamics. NACA-1119, 1953.

[75] G.M. Graham, Aeroelastic Reciprocity: An Indicial Response Formulation. AFOSR-TR-95, 1995.

[76] M.W. Kutta, Auftriebskräfte in Strömenden Flüssigkeiten. *Illustrierte Aeronautische Mitteilungen*, **6** (**133**), 1902.

[77] N.E. Joukowski, Sur les Tourbillons Adjionts. *Traraux de la Section Physique de la Societé Imperiale des Amis des Sciences Naturales*, **13** (**2**), 1906.

[78] L. Prandtl, Applications of Modern Hydrodynamics to Aeronautics. NACA TR-116, 1921.

[79] F.B. Hildebrand, A Least-Squares Procedure for the Solution of the Lifting-Line Integral Equation. NACA TN 925, 1944.

[80] D. Mateescu, et al., Theoretical Solutions for Finite-Span Wings of Arbitrary Shapes Using Velocity Singularities. *Journal of Aircraft*, **40** (**3**), 2003.

[81] T. Van Holten, Some Notes on Unsteady Lifting-Line Theory. *Journal of Fluid Mechanics*, **77** (**3**), 1976.

[82] P.D. Sclavounos, An Unsteady Lifting-Line Theory. *Journal of Engineering Mathematics*, **21** (**3**), 1987.

[83] J.L. Guermond, A. Sellier, A Unified Unsteady Lifting-Line Theory. *Journal of Fluid Mechanics*, **229**, 1991.

[84] C.D. Wieseman, Methodology for Matching Experimental and Computational Aerodynamic Data. NASA TM-100592, 1988.

[85] J. Brink-Spalink, J.M. Bruns, Correction of Unsteady Aerodynamic Influence Coefficients Using Experimental or CFD Data. AIAA-2000-1489, 2000.

[86] R. Palacios, et al., Assessment of Strategies for Correcting Linear Unsteady Aerodynamics Using CFD or Test Results. *Proceedings of the 9th IFASD*, 2001.

[87] D. Dimitrov, R. Thormann, DLM-Correction Method for Aerodynamic Gust Response Prediction. *Proceedings of the 15th IFASD*, 2013.

[88] E. Albano, W.P. Rodden, A Doublet-Lattice Method for Calculating the Lift Distribution of Oscillating Surfaces in Subsonic Flows. *AIAA Journal*, **7** (**2**), 1969.

[89] W.P. Rodden, *Theoretical and Computational Aeroelasticity*. Crest Pub., 2011.

[90] T.J. Chung, *Computational Fluid Dynamics*. Cambridge Press, 2002.

[91] C.D. Cone, The Theory of Induced Lift and Minimum Induced Drag of Non-Planar Lifting Systems. NASA TR R-139, 1962.

[92] L. Demasi, et al., An Invariant Formulation for the Minimum Induced Drag Conditions of Non-Planar Wing Systems. AIAA-2014-0901, 2014.

[93] G. Thwapiah, L.F. Campanile, Nonlinear Aeroelastic Behavior of Compliant Aerofoils. *Smart Materials and Structures*, **19** (**3**), 2010.

[94] E.H. Dowell, et al., *A Modern Course in Aeroelasticity*. Kluwer, 2004.

[95] W. Young, et al., *Roark's Formulas for Stress and Strain*. McGraw-Hill, 2011.

[96] P.D. Dunning, et al., Aeroelastic Tailoring of a Plate Wing with Functionally Graded Materials. *Journal of Fluids and Structures*, **51**, 2014.

[97] R. Cook, et al., *Concepts and Applications of Finite Element Analysis*. John Wiley & Sons, New York, 2002.

[98] M. Blair, A Compilation for the Mathematics Leading to the Doublet Lattice Method. WL-TR-92-3028, USAF, 1992.

[99] K. Appa, Finite-Surface Spline. *Journal of Aircraft*, **26** (**5**), 1989.

[100] W. Rodden, et al., Aeroelastic Addition to NASTRAN. NASA CR-3094, 1979.

[101] L.H. van Zyl, Aeroelastic Divergence and Aerodynamic Lag Roots. *Journal of Aircraft*, **38** (**3**), 2001.

[102] L.H. van Zyl, Use of Eigenvectors in the Solution of the Flutter Equation. *Journal of Aircraft*, **30** (**4**), 1993.

[103] M. Berci, Lift-Deficiency Functions of Elliptical Wings in Incompressible Potential Flow: Jones's Theory Revisited. *Journal of Aircraft*, **53** (**2**), 2016.

APPENDIX A: GENERALISED STRUCTURAL MATRICES

A.1 Plate Model

The generalised structural matrices for plate model may suitably be partitioned as:

$$\mathbf{M}^s = \begin{bmatrix} \mathbf{M}^s_{\varepsilon\varepsilon} & \mathbf{0} \\ \mathbf{0} & \mathbf{0} \end{bmatrix}, \qquad \mathbf{C}^s = \begin{bmatrix} \mathbf{C}^s_{\varepsilon\varepsilon} & \mathbf{0} \\ \mathbf{0} & \mathbf{0} \end{bmatrix}, \qquad \mathbf{K}^s = \begin{bmatrix} \mathbf{K}^s_{\varepsilon\varepsilon} & \mathbf{0} \\ \mathbf{0} & \mathbf{0} \end{bmatrix}, \tag{A1}$$

where the generalised structural mass submatrix is:

$$\mathbf{M}^s_{\varepsilon\varepsilon} = \int_0^l \int_{-b}^{b} m\boldsymbol{\phi}\boldsymbol{\phi} dxdy + \int_0^l \int_{-b}^{b} \mu_x \boldsymbol{\phi}^* \boldsymbol{\phi}^* dxdy + \int_0^l \int_{-b}^{b} \mu_y \boldsymbol{\phi}' \boldsymbol{\phi}' dxdy , \tag{A2}$$

whereas the generalised structural damping submatrix is:

$$\mathbf{C}^s_{\varepsilon\varepsilon} = \int_0^l \int_{-b}^{b} \xi\boldsymbol{\phi}\boldsymbol{\phi} dxdy , \tag{A3}$$

and the generalised structural stiffness submatrix is:

$$\begin{aligned} \mathbf{K}^s_{\varepsilon\varepsilon} = &\int_0^l \int_{-b}^{b} EI_x \boldsymbol{\phi}^{**} \boldsymbol{\phi}^{**} dxdy + \int_0^l \int_{-b}^{b} EI_{xy} \boldsymbol{\phi}^{**} \boldsymbol{\phi}'' dxdy + \int_0^l \int_{-b}^{b} EI_{yx} \boldsymbol{\phi}'' \boldsymbol{\phi}^{**} dxdy + \int_0^l \int_{-b}^{b} EI_y \boldsymbol{\phi}'' \boldsymbol{\phi}'' dxdy + \\ &+ \int_0^l \int_{-b}^{b} \overline{T}_x \boldsymbol{\phi}^* \boldsymbol{\phi}^* dxdy + \int_0^l \int_{-b}^{b} \overline{T}_{xy} \boldsymbol{\phi}^* \boldsymbol{\phi}' dxdy + \int_0^l \int_{-b}^{b} \overline{T}_{yx} \boldsymbol{\phi}' \boldsymbol{\phi}^* dxdy + \int_0^l \int_{-b}^{b} \overline{T}_y \boldsymbol{\phi}' \boldsymbol{\phi}' dxdy + \\ &+ \int_0^l \int_{-b}^{b} GJ_{xy} \boldsymbol{\phi}'^* \boldsymbol{\phi}'^* dxdy . \end{aligned} \tag{A4}$$

A.2 Beam Model

The generalised structural matrices for beam model may suitably be partitioned as:

$$\mathbf{M}^s = \begin{bmatrix} \mathbf{M}^s_{\varepsilon\varepsilon} & \mathbf{M}^s_{\varepsilon\eta} & \mathbf{0} \\ \mathbf{M}^s_{\eta\varepsilon} & \mathbf{M}^s_{\eta\eta} & \mathbf{0} \\ \mathbf{0} & \mathbf{0} & \mathbf{0} \end{bmatrix}, \qquad \mathbf{C}^s = \begin{bmatrix} \mathbf{C}^s_{\varepsilon\varepsilon} & \mathbf{0} & \mathbf{0} \\ \mathbf{0} & \mathbf{C}^s_{\eta\eta} & \mathbf{0} \\ \mathbf{0} & \mathbf{0} & \mathbf{0} \end{bmatrix}, \qquad \mathbf{K}^s = \begin{bmatrix} \mathbf{K}^s_{\varepsilon\varepsilon} & \mathbf{0} & \mathbf{0} \\ \mathbf{0} & \mathbf{K}^s_{\eta\eta} & \mathbf{0} \\ \mathbf{0} & \mathbf{0} & \mathbf{0} \end{bmatrix}, \tag{A5}$$

where the generalised structural mass submatrices are:

$$\mathbf{M}^{s}_{\varepsilon\varepsilon}=\int_0^l m\boldsymbol{\phi}\boldsymbol{\phi}dy+\int_0^l \mu_\zeta \boldsymbol{\phi}'\boldsymbol{\phi}'dy,\qquad \mathbf{M}^{s}_{\eta\eta}=\int_0^l \left(\mu_\vartheta+mx^2_{CG}\right)\boldsymbol{\varphi}\boldsymbol{\varphi}dy+\int_0^l \mu_\zeta x^2_{CG}\boldsymbol{\varphi}'\boldsymbol{\varphi}'dy,$$
$$\mathbf{M}^{s}_{\varepsilon\eta}=-\int_0^l mx_{CG}\boldsymbol{\phi}\boldsymbol{\varphi}dy-\int_0^l \mu_\zeta x_{CG}\boldsymbol{\phi}'\boldsymbol{\varphi}'dy,\qquad \mathbf{M}^{s}_{\eta\varepsilon}=-\int_0^l mx_{CG}\boldsymbol{\varphi}\boldsymbol{\phi}dy-\int_0^l \mu_\zeta x_{CG}\boldsymbol{\varphi}'\boldsymbol{\phi}'dy, \tag{A6}$$

whereas the generalised structural damping submatrices are:

$$\mathbf{C}^{s}_{\varepsilon\varepsilon}=\int_0^l \xi_\zeta\boldsymbol{\phi}\boldsymbol{\phi}dy,\qquad \mathbf{C}^{s}_{\eta\eta}=\int_0^l \xi_\vartheta\boldsymbol{\varphi}\boldsymbol{\varphi}dy, \tag{A7}$$

and the generalised structural stiffness submatrices are:

$$\mathbf{K}^{s}_{\varepsilon\varepsilon}=\int_0^l EI\boldsymbol{\phi}''\boldsymbol{\phi}''dy+\int_0^l \bar{T}\boldsymbol{\phi}'\boldsymbol{\phi}'dy,\qquad \mathbf{K}^{s}_{\eta\eta}=\int_0^l GJ\boldsymbol{\varphi}'\boldsymbol{\varphi}'dy. \tag{A8}$$

APPENDIX B: LIFT-DEFICIENCY FUNCTIONS FOR FINITE WINGS

B.1 Elliptical Wing

In general, the chord, surface and aspect ratio of flat elliptical wings are given by:

$$c=c_R\sqrt{1-\frac{y^2}{l^2}},\qquad S=\frac{\pi l c_R}{2},\qquad AR=\frac{8l}{\pi c_R}, \tag{B1}$$

respectively, with c_R the root chord; in particular, the latter is conveniently chosen as $c_R=2$ without loss of generality in the subsequent analysis [20,22,103].

B.1.1. Unit Step-Change in the Angle of Attack

Coherently assuming an ideal elliptical loading due to a suitable distribution of elementary vortex loops, the wing's lift-deficiency coefficient $C^{3D}_{L\alpha}(\tau)$ and circulation $\Gamma^{3D}_w(\tau)$ from a unit step in the angle of attack are written along with the tips-induced downwash $V_w(\tau)$ as [20]:

$$\begin{aligned}
C^{3D}_{L\alpha}&=C^{2D}_{L\alpha}-\pi V_w+\int_0^\tau \frac{dC^{2D}_{L\alpha}(\tau-\iota)}{d\iota}V_w(\iota)d\iota,\\
\Gamma^{3D}_w&=\Gamma^{2D}_w+\int_0^\tau \frac{d\Gamma^{2D}_w(\tau-\iota)}{d\iota}V_w(\iota)d\iota,\\
V_w&=\Gamma^{3D}_w V_{\Gamma 0}-\int_0^\tau \frac{dV_\Gamma(\tau-\iota)}{d\iota}\Gamma^{3D}_w(\iota)d\iota,
\end{aligned} \tag{B2}$$

where $C_{L\alpha}^{2D}(\tau)$ and $\Gamma_w^{2D}(\tau)$ are the lift-deficiency coefficient and related circulation given by Wagner and Kussner functions for a two-dimensional flat aerofoil (which account for the inflow generated by the travelling wake), respectively [23-25]:

$$C_{L\alpha}^{2D} = \int_{-\infty}^{+\infty}\left(\frac{\mathrm{C}}{\mathrm{jk}}\right)e^{\mathrm{jk}\tau}d\mathrm{k}\,, \qquad \Gamma_w^{2D} = \int_{-\infty}^{+\infty}\left(\frac{\mathrm{C_G}}{\mathrm{jk}}\right)e^{\mathrm{jk}\tau}d\mathrm{k}\,, \tag{B3}$$

whereas Theodorsen $\mathrm{C}(\mathrm{k})$ and (modified) Sears $\mathrm{C_G}(\mathrm{k})$ functions are defined as [26-28]:

$$\mathrm{C} = \frac{H_1^{(2)}}{H_1^{(2)} + \mathrm{j}H_0^{(2)}}\,, \qquad \mathrm{C_G} = \left[\mathrm{C}\left(B_0^{(1)} - \mathrm{j}B_1^{(1)}\right) + \mathrm{j}B_1^{(1)}\right]e^{-\mathrm{jk}}\,, \tag{B4}$$

with $H_n^{(2)}(\mathrm{k}) = B_n^{(1)}(\mathrm{k}) - \mathrm{j}B_n^{(2)}(\mathrm{k})$ Hankel functions of the second type and n-th order while $B_n^{(1)}(\mathrm{k})$ and $B_n^{(2)}(\mathrm{k})$ Bessel functions of the first and second type and n-th order [41].

The gradient of the wing downwash $V_\Gamma(\tau)$ with respect to the wing circulation due to a series of vortex loops extending along the wake reads [22]:

$$V_\Gamma = \frac{2}{\pi^2 AR}\left\{\left(\frac{4x_w}{\pi AR}\right)s_w K + \left(\frac{\pi AR}{4x_w}\right)\left[\left(s_w - \frac{1}{s_w}\right)K + \frac{E}{s_w} - 1\right]\right\}, \tag{B5}$$

where $K(s_w)$ and $E(s_w)$ are the elliptic integrals of the first and second kind [20], respectively, whereas the non-dimensional wake development $x_w(\tau)$ and $s_w(\tau)$ are readily given by the two-dimensional theory via Joukowski transform as [20,103]:

$$x_w = \sqrt{\tau(2+\tau)}\,, \qquad s_w = \left[1 + \left(\frac{4x_w}{\pi AR}\right)^2\right]^{-\frac{1}{2}}\,, \tag{B6}$$

being $x_w \approx 1 + \tau$ for $\tau > 2$ with excellent accuracy; yet, note that $\lim_{\tau\to 0} x_w = 0$ and $\lim_{\tau\to 0} s_w = 1$.

The sectional lift-deficiency coefficient, the related circulation and the wing's downwash gradient may then be approximated as [22,103]:

$$\begin{aligned}
C_{L\alpha}^{2D} &= 2\pi\left(1 - \sum_{j=1}^{n^C} A_j^C e^{-B_j^C\tau}\right), & \sum_{j=1}^{n^C} A_j^C &= \frac{1}{2}, \\
\Gamma_w^{2D} &= 2\pi\left(1 - \sum_{j=1}^{n^\Gamma} A_j^\Gamma e^{-B_j^\Gamma\tau}\right), & \sum_{j=1}^{n^\Gamma} A_j^\Gamma &= 1, \\
V_\Gamma &= \frac{1}{\pi AR}\left(1 - \sum_{j=1}^{n^V} A_j^V e^{-B_j^V\frac{(\tau-\tau_0)}{AR}}\right), & \sum_{j=1}^{n^V} A_j^V &= 1,
\end{aligned} \tag{B7}$$

where all coefficients A_j^C, A_j^Γ, A_j^V and B_j^C, B_j^Γ, B_j^V are obtained by constrained nonlinear fitting of the exact curves; finally, the time shift $\tau_0 = -\frac{\pi}{2}$ accounts for the initial wake length being set equal to the mean geometric chord and complying with the unsteady realisation of Kutta condition [20,21]. Due to Laplace transformation, the integral convolution process can thus be written as [22]:

$$\begin{aligned} C_{L\alpha}^{3D} &= C_{L\alpha}^{2D} - \pi V_w - 2\pi \sum_{j=1}^{n^C} A_j^C z_j^C \,, \\ \Gamma_w^{3D} &= \Gamma_w^{2D} - 2\pi \sum_{j=1}^{n^\Gamma} A_j^\Gamma z_j^\Gamma \,, \\ V_w &= \Gamma_w^{3D} V_{\Gamma 0} + \frac{1}{\pi AR} \sum_{j=1}^{n^V} A_j^V e^{-\frac{\pi B_j^V}{2AR}} z_j^V \,, \end{aligned} \tag{B8}$$

where the added aerodynamic states $z_j^C(\tau)$, $z_j^\Gamma(\tau)$ and $z_j^V(\tau)$ evolve as:

$$\frac{dz_j^C}{d\tau} + B_j^C z_j^C = B_j^C V_w \qquad \frac{dz_j^\Gamma}{d\tau} + B_j^\Gamma z_j^\Gamma = B_j^\Gamma V_w \,, \qquad \frac{dz_j^V}{d\tau} + \frac{B_j^V z_j^V}{AR} = \frac{B_j^V \Gamma_w^{3D}}{AR} \,, \tag{B9}$$

from the initial conditions $z_j^C(0) = 0$, $z_j^\Gamma(0) = 0$ and $z_j^V(0) = 0$.

As the asymptotic (steady) condition is in exact agreement with lifting line theory [78] (i.e., the downwash angle is constant and the load-scaling function κ is unitary along the span), the numerically integrated wing's lift-deficiency coefficient may finally be approximated as [103]:

$$C_{L\alpha}^{3D} = \frac{2\pi AR}{2+AR} \left\{ 1 - \left[\frac{(2E-1)AR - 2}{(AR-2)E} \right] \sum_{j=1}^{n} A_j e^{-B_j \tau} \right\}, \qquad \sum_{j=1}^{n} A_j = 1 - \frac{2+AR}{2AR} \,, \tag{B10}$$

where the n coefficients A_j and B_j are still derived from constrained nonlinear curve-fitting [69]. Alternatively to employing a further exponential term [103], the proposed approximation has inherently been tuned to satisfy Kutta-Joukowsky condition at the impulsive start of the wake, since the latter initially moves as an "extension" of the wing and the resulting apparent flow inertia is obtained by considering the pressure difference $\Delta p(x,\tau)$ due to the kinetic flow potential $\Pi(x,\tau)$ over each two-dimensional wing section in normal motion, namely [20]:

$$\Pi = \frac{V_w}{E} \sqrt{(1+x)(1-x+\tau)} \,, \qquad \Delta p = -2\rho U \left(\frac{\partial \Pi}{\partial \tau} + \frac{\partial \Pi}{\partial x} \right), \tag{B11}$$

the net variations of which being due to the apparent change in the wing shape. The impulsive pressure distribution is then instantaneously integrated over the elliptic planform (neglecting the variation of its perimeter is during the apparent widening), so that the initial and final limits of the wing load are effectively obtained by scaling those of the aerofoil load as [22,103]:

$$\lim_{\tau\to 0} C_{L\alpha}^{3D} = \frac{2\pi}{E}, \qquad \lim_{\tau\to\infty} C_{L\alpha}^{3D} = \frac{2\pi AR}{2+AR}. \tag{B12}$$

In summary, the initial wing lift is slightly less than that of the isolated aerofoil (due to inertia effect), whereas the asymptotic steady lift may be considerably less (due to downwash effect) in the case of a small aspect ratio. Note that the lift-deficiency functions of the flat airfoil already account for the wake vortex's inflow (including the gust penetration effect), while the downwash induced by the wing-tip vortices modifies the effective angle of attack; moreover, the latter "becomes practically uniform over the entire wing span before the wake has attained a length of the order of one semispan" [20] and the initial lift distribution is hence similar to the final one. In essence, this model relies on physical assumptions and applicability conditions comprising those of both two-dimensional unsteady and three-dimensional steady incompressible potential flow; therefore, provided appropriate approximations are employed for all its basic elements, its accuracy increases with increasing wing's aspect ratio. Finally, strip theory is correctly resumed in the case of infinite wing, where $C_{L\alpha}^{3D} \approx C_{L\alpha}^{2D}$ (i.e., Wagner function) and $\Gamma_w^{3D} \approx \Gamma_w^{2D}$ (i.e., Kussner function) with $V_\Gamma \approx 0$ and $E \approx 1$ for $AR \to \infty$ [103].

B.1.2. Unit Sharp-Edge Vertical Wind Gust

Due to the progressive penetration of the vertical wind gust with a "frozen" approach [42], the initial perturbations of both flow potential and tip-vortices strength are small; therefore, the wing lift starts at zero and increases with theoretically infinite rate [20]. Although all wing sections are assumed to enter the gust simultaneously and even if both Kussner function for the aerofoil lift and Sears function for the related circulation correctly embed the gust penetration effect, the flow inertia resulting from the impulsive start of the wake may also be important for wings with small aspect ratio. The lift-deficiency coefficient $C_{LG}^{3D}(\tau)$ from a unit sharp-edge gust may then be obtained from a generalisation of its reciprocal relation [73-75] with the wing's lift-deficiency coefficient from a unit step in the angle of attack directly [103]:

$$C_{LG}^{3D} = \begin{cases} \displaystyle\int_0^\tau C_{L\alpha}^{3D}(\tau-\iota)\sqrt{\frac{\iota}{2-\iota}}\frac{d\iota}{\pi} + \frac{2}{E}\sqrt{\tau(2-\tau)}, & 0 \le \tau \le 2, \\ \displaystyle\int_0^2 C_{L\alpha}^{3D}(\tau-\iota)\sqrt{\frac{\iota}{2-\iota}}\frac{d\iota}{\pi}, & \tau \ge 2, \end{cases} \tag{B13}$$

where $\tau = 2$ is the reduced time taken by the gust to impinge the entire root chord [20,22,103].

B.2 Trapezoidal Wing

The chord, surface and aspect ratio of flat trapezoidal wings are given by:

$$c = c_R\left[1-(1-\lambda)\frac{y}{l}\right], \qquad S = (1+\lambda)lc_R, \qquad AR = \frac{4l}{(1+\lambda)c_R}, \tag{B14}$$

respectively, where $0 \le \lambda \le 1$ is the taper ratio (i.e., the ratio between tip and root chords) [22].

B.2.1. Unit Step-Change in the Angle of Attack

With an effective simplified approach, a single vortex-ring is considered for modeling the total (lumped) wing circulation [21]. The bound vortex is placed at the quarter chord, where the aerodynamic centre of each section is assumed in accordance with thin airfoil theory, while the wing-tip vortices are trailed parallel to the free-stream; a single control point for the total downwash is then consistently placed at the third quarter of the wing's root chord, where the flow's non-penetration boundary condition is satisfied [38]. All vortices have the same (lumped) intensity and the shed vorticity travels towards infinity with half the reference speed from half the wing's root chord behind the control point [21], hence stretching the vortex-ring and increasing the wake length; when the wing wake eventually approaches infinity, its influence on the wing flow fades away and the steady condition is asymptotically obtained. The influence of both tip vortices and unsteady wake on the wing lift is thus calculated with the simplest implementation of unsteady lifting line theory [81-83] and the total load build-up is obtained as function of both aspect and taper ratios.

Considering all contributions due to bound, trailed and shed vortices of the vortex-ring, the lift-deficiency coefficient from a unit step in the angle of attack is then calculated based on Kutta-Joukowsky theorem and Biot-Savart law as [21-22]:

$$C_{L\alpha}^{3D} = \frac{2\pi AR_e}{\sqrt{1+AR_e^2}+\dfrac{2}{2+\tau}\sqrt{\left(1+\dfrac{\tau}{2}\right)^2+AR_e^2}}, \qquad AR_e = \left(\frac{1+\lambda}{2}\right)AR, \tag{B15}$$

with initial (impulsive) and asymptotic (steady) behaviours respectively given by [22]:

$$\lim_{\tau\to 0} C_{L\alpha}^{3D} = \frac{\pi AR_e}{\sqrt{1+AR_e^2}}, \qquad \lim_{\tau\to \infty} C_{L\alpha}^{3D} = \frac{2\pi AR_e}{1+\sqrt{1+AR_e^2}}, \tag{B16}$$

which correctly resume Garrick's approximation [73] of Wagner function for thin airfoils, in the limit of infinitely slender wing for $AR_e \to \infty$. However, due to the inherent limitations of the simple vortex-system employed, these initial and final values of the lift coefficient are not accurate and shall rather be provided by other higher-fidelity sources [88-90], suitable approximate expressions being [17,22]:

$$C_{L0}^{3D} = \frac{\pi AR_e}{E\sqrt{1+AR_e^2}}, \qquad C_{L\infty}^{3D} = \frac{2\pi AR_e}{2(1+e)+AR_e}, \tag{B17}$$

with $e > 0$ an appropriate efficiency factor (being $e = 0$ for elliptical planform). The wing's lift-deficiency coefficient may hence finally be approximated as [22]:

$$C_{L\alpha}^{3D} = \frac{2\pi AR_e}{2(1+e)+AR_e}\left\{1-\left[\frac{2E\sqrt{1+AR_e^2}-AR_e-2(1+e)}{\left(\sqrt{1+AR_e^2}-1\right)E}\right]\sum_{j=1}^{n} A_j e^{-B_j\tau}\right\}, \qquad \sum_{j=1}^{n} A_j = \frac{1}{2}\left(1-\frac{1}{\sqrt{1+AR_e^2}}\right), \tag{B18}$$

where all coefficients A_j and B_j are obtained by constrained nonlinear fitting of the "exact" curve [69], while both the asymptotic $C_{L\infty}^{3D} = \lim_{\tau\to\infty} C_{L\alpha}^{3D}$ and the initial $C_{L0}^{3D} = \lim_{\tau\to 0} C_{L\alpha}^{3D}$ conditions are automatically satisfied. Note that the proposed model is indeed better suited for thin slender wings with high aspect and taper ratios, for which the three-dimensional flow and geometry effects are less significant (i.e., the induced downwash is smaller and the control point of each wing section is closer to the root one).

B.2.2. Unit Sharp-Edge Vertical Wind Gust

In order to obtain the lift-deficiency coefficient from a unit sharp-edge vertical wind gust with the standard "frozen" approach [42], that from a unit step in the angle of attack is convolved with the fictitious angle of attack $\theta(\tau)$ derived from the Fourier transform of the ratio between Sears and Theodorsen functions (which represents a delay function [73-75] for two-dimensional flow), namely [22]:

$$C_{LG}^{3D} = \int_0^{\tau} C_{L\alpha}^{3D}(\tau - \iota)\theta(\iota)d\iota\,, \qquad \theta = \frac{1}{2\pi}\int_{-\infty}^{+\infty}\left(\frac{\mathrm{C_G}}{\mathrm{C}}\right)\frac{e^{\mathrm{j}\mathrm{k}\tau}}{\mathrm{j}\mathrm{k}}d\mathrm{k}\,; \tag{B19}$$

this is substantially equivalent to multiplying the lift-deficiency coefficient from a unit step in the angle of attack by the ratio between Kussner and Wagner functions (which approximates the two-dimensional effect of the gust penetration, assuming that all wing sections encounter the gust at the same time).

Note that the gust penetration delays the circulation growth and hence reaching the asymptotic (steady) lift [17,22], which coincides with that from a unit step in the angle of attack; also, Kussner function for thin airfoils is correctly resumed in the limit of infinite wing.